

General Disclaimer

One or more of the Following Statements may affect this Document

- This document has been reproduced from the best copy furnished by the organizational source. It is being released in the interest of making available as much information as possible.
- This document may contain data, which exceeds the sheet parameters. It was furnished in this condition by the organizational source and is the best copy available.
- This document may contain tone-on-tone or color graphs, charts and/or pictures, which have been reproduced in black and white.
- This document is paginated as submitted by the original source.
- Portions of this document are not fully legible due to the historical nature of some of the material. However, it is the best reproduction available from the original submission.

(NASA-TM-73715) FERROGRAPHIC ANALYSIS OF
WEAR DEBRIS GENERATED IN ACCELERATED ROLLING
ELEMENT FATIGUE TESTS (NASA) 22 p HC A02/MP
A01 CSCI 11F

N77-32288

Unclass
49090

G3/26

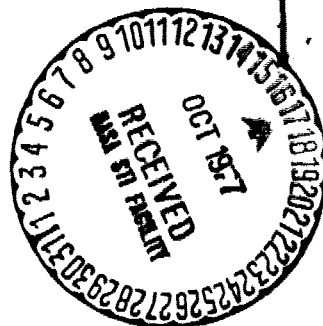
NASA TECHNICAL MEMORANDUM

NASA TM 73715

NASA TM 73715

FERROGRAPHIC ANALYSIS OF WEAR DEBRIS GENERATED IN ACCELERATED ROLLING ELEMENT FATIGUE TESTS

by William R. Jones, Jr. and Richard J. Parker
Lewis Research Center
Cleveland, Ohio 44135



TECHNICAL PAPER to be presented at the
Joint Lubrication Conference
cosponsored by the American Society of Lubrication Engineers
and the American Society of Mechanical Engineers
Kansas City, Missouri, October 3-5, 1977

FERROGRAPHIC ANALYSIS OF WEAR DEBRIS GENERATED IN ACCELERATED ROLLING ELEMENT FATIGUE TESTS

by William R. Jones, Jr. and Richard J. Parker

National Aeronautics and Space Administration
Lewis Research Center
Cleveland, Ohio 44135

ABSTRACT

Ferrographic analysis was used to determine the types and quantities of wear particles generated during accelerated rolling contact fatigue tests. The NASA five-ball rolling contact fatigue tester was used. Ball specimens were made of AMS 5749, a corrosion resistant, high-temperature bearing steel. The lubricant was a super-refined naphthenic mineral oil. Conditions included a maximum Hertz stress of 5.52×10^9 Pa and a shaft speed of 10 000 rpm. Four types of wear particles were observed; normal rubbing wear particles, fatigue spall particles, spheres, and friction polymer.

INTRODUCTION

The goals of oil analysis are to diagnose the current state of health of operating machines and to be able to predict any future problems. A variety of different techniques (1) are being employed to effect these goals. These include: spectrometric oil analysis (SOAP), magnetic chip detectors, vibration sensors, and particle counters. Each of these techniques have certain advantages, but most suffer from the disadvantage of not being able to distinguish between the various wear modes that can occur.

A new instrument, the Ferrograph, has been developed which magnetically precipitates wear debris from used lubricants onto a glass slide to yield a Ferrogram (2 to 4). The precipitated particles range in size from approximately 0.02 to a few micrometers and are arranged according to size on the slide. Individual particles may be observed with a unique bichromatic microscope, the Ferroscope, or with a conventional scanning electron microscope.

A number of investigators (5 to 10) have identified the characteristic wear particles associated with the various wear mechanisms. In particular, three distinct

particle types have been related to rolling contact fatigue: spheres, spall, and laminar particles (10). Indeed the occurrence of spherical particles in oil samples has been shown to be a precursor of bearing fatigue in some cases (9, 10, 11).

The objective of this investigation was to use the Ferrograph to determine the types and quantities of wear particles generated during accelerated rolling-contact fatigue tests. Test materials were AMS 5749 steel balls and a super-refined naphthenic mineral oil. Tests were conducted in the NASA five-ball fatigue tester at a maximum Hertz stress of 5.52×10^9 Pa (800 000 psi), a contact angle of 30° , a shaft speed of 10 000 rpm, and a temperature of 340 K (150° F).

EXPERIMENTAL APPARATUS AND PROCEDURE

Five-Ball Fatigue Tester

The NASA five-ball fatigue tester was used for all tests. The apparatus is described in detail in reference 12. The five-ball test assembly is shown in figure 1. This fatigue tester consists essentially of an upper test ball pyramided upon four lower balls that are positioned by a separator and are free to rotate in an angular-contact raceway. System loading and drive are supplied through a vertical drive shaft, which grips the upper-test ball. For every revolution of the drive shaft, the upper-test ball receives three stress cycles from the lower balls. The upper-test ball and raceway are analogous in operation to the inner and outer races of a bearing, respectively. The separator and lower balls function in a manner similar to the cage and the balls in a bearing.

The 1.27-cm- (1/2-in.-) diameter, grade 10, VIM-VAR AMS 5749 steel balls used in these tests were from a single heat of material. A typical chemical analysis (wt %) of this material is as follows: C, 1.15; Si, 0.30; Mn, 0.50; Cr, 14.5; Mo, 4.0; V, 1.2; and the balance Fe.

Lubrication is provided by a once-through, mist lubrication system. The lubricant was a super-refined naphthenic mineral oil with a viscosity of 79×10^{-6} m²/sec (79 cS) at 311 K (100° F). Vibration instrumentation detects a fatigue spall on either the upper or the lower ball and automatically shuts down the tester. This provision allows unmonitored operation and a consistent criterion for failure. The test assem-

bly is blanketed with nitrogen during operation. Tests were conducted at a maximum Hertz stress of 5.52×10^9 Pa (800 000 psi). This higher than normal stress accelerates the fatigue process so that data may be obtained in a reasonable length of time.

Fatigue Testing Procedure

Before they were assembled in the five-ball fatigue tester, all test-section components were flushed and scrubbed with ethyl alcohol and wiped dry with clean cheesecloth. The test assembly was coated with lubricant to prevent wear at startup. A new set of five balls was used for each test. Each test was suspended when a fatigue failure occurred on either a lower or an upper test ball or when a preset cutoff time was reached. The speed, outer-race temperature, and oil flow were monitored and recorded at regular intervals. After each test, the outer race of the five-ball system was examined visually for damage. If any damage was discovered, the race would be replaced before further testing.

Ferrograph

The Ferrograph (2 to 4) is an instrument used to magnetically precipitate wear particles from a used oil onto a specially prepared glass slide. A mixture of 3×10^{-6} cubic meter (3 ml) of used oil and 1×10^{-6} cubic meter (1 ml) of solvent is prepared. This mixture is then slowly pumped over the slide as shown in figure 2. A wash and drying cycle follows which removes residual oil and permanently attaches the particles to the slide. The resulting slide with its associated particles is called a Ferrogram.

The amount of wear debris on a Ferrogram was determined by measuring the optical density (percent area covered) of the deposit at seven positions along the slide, entry, 54, 50, 40, 30, 20, and 10 mm. A composite Ferrogram density was determined for each set of conditions by averaging the seven readings.

Sample Collecting Procedure

The five-ball fatigue tester is mist-lubricated in a once-through system by a very small quantity of lubricant (<0.5 ml/hr). Samples (~ 5 ml) were collected periodically from the gravity drain tube below the tester. Sample times were somewhat erratic

because of the low and sometimes varying mist flow rate and because the rig was unattended overnight.

RESULTS AND DISCUSSION

The oil samples analyzed in this study were obtained from two series of tests included in a larger fatigue test program reported in reference 13. The two test series included a total of 52 fatigue tests, 16 of which were monitored by Ferrography. Of these 16 tests, fatigue failures occurred in 7 of them after test durations ranging from 22 to 98 hours. The remaining 9 tests were suspensions. If a fatigue failure had not occurred by a certain preset time (~ 100 hr), the test was terminated. Test times for the suspensions ranged from 100 to 118 hours. In this study, the tests resulting in failure will be designated as F-1, F-2, etc., and the suspensions as S-1, S-2, etc. A typical fatigue spall is shown in figure 3(a). An enlarged area of the spall appears in figure 3(b). The massive (~ 0.1 mm in major dimension) spall particles resulting from the failure are easily visible.

Wear Particle Types

Although a variety of different kinds of wear particles were observed in this study, only four types consistently appeared in most samples. These types were: normal rubbing wear particles, fatigue spall particles, spherical particles and friction polymer. Table I contains a summary of the wear particle types observed in this study. Three of these types are evident in figure 4 which is an optical micrograph of the Ferrogram entry deposit from test F-6 (76 hr sample).

Normal Rubbing Wear Particles

Oil samples from almost any source contain some normal rubbing wear particles. This particle type normally represents a benign form of wear and most samples in this study contained at least a few such particles. These particles consist of small ($<5 \mu\text{m}$ in major dimension and $<1 \mu\text{m}$ thick) asymmetrical metallic flakes. When many of these particles are present in a sample, they will appear as strings on the Ferrograms due to alignment by the magnetic field. An electron micrograph of such a string of normal rubbing wear particles appears in figure 5(a). These particles were in the oil sampled at the conclusion of the 98 hour test, F-7. Energy-dispersive

X-ray analysis (EDAX) of the particle labelled A in figure 5(a) is shown in figure 5(b). The analysis indicates that the particle is from the bearing steel test specimens. Figure 5(c) contains the background EDAX analysis for the Ferrogram slide. In addition, most Ferrograms were gold-plated prior to analysis.

Fatigue Spall Particles

As one would expect, fatigue spall particles were observed on many Ferrograms. However, these particles are not to be confused with the massive spall particles occurring at failure and shown in figure 3(b). These macroscopic (tenths of millimeters in major dimension) spall fragments were not observed in this study. This is to be expected since the rig and lubricant flow are shut down immediately as a spall occurs.

However, prior to fatigue failure and as the major spall is developing, microspall particles are generated. Typically, these particles were 5 to 20 μm in length and 1 to 2 μm in thickness. They appeared as flat platelets having smooth surfaces and irregular shapes. Examples appear in figure 4.

Spherical Particles

Metallic microspheres (1 to 10 μm in diameter) were observed in most samples. However, most of the spheres were less than 5 μm in diameter. An electron micrograph of a sphere appears in figure 6(a). Typical EDAX analyses for the spherical particles appear in figures 6(b) and (c). As can be seen the spheres were composed of either Mn and Fe or Fe, Cr, V, Mo, and Mn. The latter, of course, corresponds to the composition of AMS 5749. The origin of the Fe and Mn spheres is not known. However it should be noted that Ferrograms prepared from unused oils will sometimes contain a few spheres. Therefore it is felt that sphere counts of less than 10 are probably not significant.

Friction Polymer

Most Ferrograms contained varying amounts of friction polymer deposits. Examples of this material are shown in figures 3 and 6(a). EDAX analysis of the deposit in figure 6(a) is given in figure 6(d). After allowing for the background elements only a small amount of Fe and Cu are contained in the deposit. The Fe is most likely from small rubbing wear particles occluded in the deposit. Unfortunately, carbon cannot

be detected by EDAX. However it is a logical assumption that the majority of the deposit must be organic in nature.

Actually two types of the friction polymer deposit were observed. These are illustrated in figure 7. The first type is an amorphous appearing deposit that is transparent when viewed with transmitted light and appears dark in reflected white light. This type was not observable when reflected polarized light was used with a crossed analyzer. The second type appears to be crystalline in nature. When viewed with reflected white light it appears light blue and is translucent to transmitted light. Under reflected polarized light viewed with a crossed analyzer, it appears white.

Both forms of deposit occurred on almost all Ferrograms. The deposits were distributed throughout the length of the Ferrograms, but the total amount varied. The deposits ranged from micron sized to several millimeters in diameter. There was no apparent correlation between the amounts of these deposits and the amount of metallic debris or sampling time. This material is continually formed during tests with the naphthenic mineral oil lubricant. However, no friction polymer was observed on any of the Ferrograms from the lower stress (3.4×10^9 Pa, 500 000 psi) test (S-9).

The material must be only partially soluble in the solvents used in preparing the Ferrograms. Conceivably, if a different solvent system is used in which the material is completely soluble, its presence on the Ferrograms could be avoided.

Friction polymer deposits have been observed on Ferrograms in other studies. Polyphenyl ethers (14) produced characteristic rock-like and cylindrical organo-metallic debris in pin-on-disk experiments. Other deposits, termed "polymud," were observed with MIL-L-23699 polyester oils in rubbing wear experiments (4).

Correlation of Ferrogram Results with Fatigue Failure

One useful technique for following a developing failure is to monitor the ratio of large to small wear particles. The ratio is determined by optically measuring the percent area covered at the entry for the large particles and at the 50 mm position for the small particles. Bowen and Westcott (10) have advocated the use of two other parameters, the general wear level parameter and the wear severity index. Both are calculated from the large and small particle measurements. All three parameters

will normally increase as failure approaches. However, none of the parameters were useful in this study because of the friction polymer deposits. The optical densitometer does not differentiate between the nonmetallic friction polymer and the metallic wear particles. Composite Ferrogram densities for each test were determined and appear in Tables II and III. However, since the composite densities also reflect the varying amounts of friction polymer, no correlation exists between the fatigue results and these measurements.

The progression of the fatigue process has been studied by other investigators (6 to 11). In those studies, a precursor to fatigue failure has been the appearance of metallic microspheres in the lubricant. In addition, microspall particles and laminar particles sometimes appear in the oil prior to failure.

It would then appear that fatigue failure should be easy to predict. However, a number of problems exist which can make prediction difficult. Metallic spheres can be generated by mechanisms other than fatigue, such as grinding (15, 16), welding (10), fretting (17), cavitation erosion (18), and possibly burnishing (19). Except for size differences, spheres from different mechanisms appear morphologically similar. Also, some rolling contact fatigue studies (20) have yielded few spheres, while others have shown that millions of spheres can be generated (11).

Another problem area is that of distinguishing between large rubbing wear particles and small fatigue spall particles. Both have similar major dimensions ($\sim 5 \mu\text{m}$) and similar morphologies. Both are thin platelets (1 to $2 \mu\text{m}$ thick) with smooth surfaces.

Bearing these problems in mind, the quantities of both particle types associated with rolling contact fatigue (spheres and microspall particles) were determined for each oil sample. Laminar particles reported by others (10) were not observed in this study. The quantity of spheres in a sample was determined by simply counting the number between approximately 50 and 55 mm on each Ferrogram. The following rating was used for the fatigue microspall particles: few (+), several (++), many (+++), and very many (+++). Although not associated with the fatigue process, the quantity of normal rubbing wear particles were rated in an identical manner. All

three values are summarized for each sample in Table II (Failures) and Table III (Suspensions). The composite Ferrogram densities and sample times also appear in these tables. As can be seen, the results were quite variable. In some instances the increase in spheres and microspall particles was dramatic (F-6, F-7, S-2, and S-3). In other cases, there was little if any increase (F-4, F-5, and S-8). However, in a majority of the tests, one or both of the parameters reached a maximum during the last one-third of the test durations.

When this study was initiated it was felt that the suspended tests would provide the control or baseline data. It was not appreciated that due to the accelerated nature of these tests, the suspensions could also be in the process of fatiguing. The types and quantities of wear debris are quite similar from both failures and suspensions. Some test balls from suspended tests were examined to see if a fatigue process was interrupted before the primary spall could occur. Upper test balls from five suspended tests were sectioned and examined optically and in a scanning electron microscope. All examined balls showed varying degrees of surface damage (i. e., minor spalls and cracks). An example of a surface crack on the ball from test S-8 (100 hr) appears in figure 8. An electron micrograph of a number of minor spalls on the ball from test S-5 (100 hr) is shown in figure 9. Balls from tests S-2, S-3, and S-6 showed similar types of surface damage.

Therefore, it was felt that a test run at a reduced stress level (3.4×10^9 Pa, 500 000 psi) would provide a better baseline for comparison. At this level, fatigue progression should be slow enough that little damage would be incurred by the test balls during a 100-hour test. Suspension S-9 run at the above reduced stress did yield different results compared to the higher stress tests. Although a few spheres were observed, there were no abrupt increases. Very few microspall particles were generated but the number of normal rubbing wear particles appeared to increase. There was also a complete absence of friction polymer deposits.

Correlation of Results with Other Investigators

Qualitatively, the results of this study correlate with the observations of others (6, 9, 10, and 11) that microspall and spherical particles are associated with rolling

contact fatigue. However, the large number of spheres ($>1000/\text{Ferrogram}$) observed by Middleton (11) was not confirmed in this study. The maximum number of spheres appearing on any one Ferrogram was about 50. In addition, laminar particles (20 to $50\text{ }\mu\text{m}$ in major dimension, $<1\text{ }\mu\text{m}$ thick) which have been associated with fatigue (10) were not observed. These discrepancies may be related to the accelerated nature of these tests.

Effect of Dissolved Water on Sphere Production

It is well known that dissolved water in a lubricant accelerates rolling contact fatigue (21). Presumably, this occurs because of water adsorption in fatigue cracks. This could lead to hydrogen embrittlement of the metal which would greatly accelerate the rate of crack propagation and thus fatigue. If the spherical particles are generated in propagating fatigue cracks, as has been theorized (9, 10, and 11), one would expect any process that accelerates crack propagation to cause a decrease in sphere production. Therefore, under similar test conditions, a "wet" lubricant may yield fewer spheres than a "dry" one during fatigue progression. In our program, no attempt was made to dry or control the moisture content of the naphthenic mineral oil. It was used in the as-received condition ($<50\text{ ppm}$ dissolved water content).

Other Observed Particle Types

Iron oxide (rust) particles and some severe wear fragments were occasionally observed on the Ferrograms. Cutting wear particles were observed in only one set of samples (S-5). None of these particle types appeared to have any connection to fatigue progression.

Predictive Capability of Ferrography

Little can be said about the predictive capability of Ferrography in regard to these tests. Their accelerated nature, greatly compressed the time scale for failures to occur. This factor combined with the low lubricant flow rate limited the number of samples for analysis.

SUMMARY OF RESULTS

The major results of the Ferrographic analysis of wear debris generated during accelerated rolling contact fatigue tests may be summarized as follows:

1. Four types of wear debris were observed:
 - a. Normal rubbing wear particles
 - b. Fatigue spall particles
 - c. Spheres
 - d. Friction polymer
2. For a majority of tests (including failures and suspensions), fatigue spall particle rating and the number of spherical particles reached a maximum during the last one-third of the test durations.
3. The number of spheres observed (<50 per 3 ml sample) in these accelerated tests was much less than others have reported during long duration testing under lower loads.
4. Laminar particles, sometimes associated with rolling contact fatigue, were not observed in this study.

ACKNOWLEDGEMENT

The authors wish to thank Mr. Vernon Westcott of Foxboro/Trans-Sonics, Inc. for his assistance in obtaining the SEM analysis. The SEM analysis was performed by the National Engineering Laboratory, East Kilbride, Glasgow.

REFERENCES

1. Beerbower, A., "Spectrometry and Other Analysis Tools for Failure Prognosis," Lubr Eng., 32, 285 (1976).
2. Seifert, W. W. and Westcott, V. C., "A Method for the Study of Wear Particles in Lubricating Oil," Wear, 21, 27 (1972).
3. Westcott, V. C., and Seifert, W. W., "Investigation of Iron Content of Lubricating Oils Using Ferrograph and Emission Spectrometer," Wear, 23, 239 (1973).
4. Scott, D., Seifert, W. W., and Westcott, V. C., "Ferrography - An Advanced Design Aid for the 80's," Wear, 34, 251 (1975).
5. Reda, A. A., Bowen, R., and Westcott, V. C., "Characteristics of Particles Generated at the Interface Between Sliding Steel Surfaces," Wear, 34, 261 (1975).

6. Scott, D., Seifert, W. W., and Westcott, V. C., "The Particles of Wear," Sci. Am., 230, 88-97 (1974).
7. Westcott, V. C. and Middleton, J. L., "The Investigation and Interpretation of the Nature of Wear Particles," Trans-Sonics, Inc. (AD-A003553), Burlington, Mass. (1974).
8. Scott, D. and Mills, G. H., "Debris Examination in the SEM: A Prognostic Approach to Failure Prevention," in Seventh Annual Symposium on Scanning Electron Microsc.: Workshop on Failure Analysis, Inst. Technol. Res. Inst., 1974, pp. 883-888.
9. Scott, D. and Mills, G. H., "Spherical Debris - Its Occurrence, Formation and Significance in Rolling Contact Fatigue," Wear, 24, 235 (1973).
10. Bowen, E. R. and Westcott, V. C., "Wear Particle Atlas," Final Report Contract N00156-74-C1687, Naval Air Engineering Center, July 1976.
11. Middleton, J. L., Westcott, V. C., and Wright, R. W., "The Number of Spherical Particles Emitted by Propagating Fatigue Crack in Rolling Bearings," Wear, 30, 275 (1974).
12. Carter, T. L., Zaretsky, E. V., and Anderson, W. J., "Effect of Hardness and Other Mechanical Properties on Rolling-Contact Fatigue Life of Four High-Temperature Bearing Steels," NASA TN D-270 (1960).
13. Parker, R. J. and Hodder, R. S., "Effect of Double Vacuum Melting and Retained Austenite on the Rolling-Element Fatigue Life of AMS 5749 Corrosion Resistant, High Temperature Bearing Steel," NASA TN (in process).
14. Jones, W. R., Jr., "Ferrographic Analysis of Wear Debris from Boundary Lubrication Experiments with a Five-Ring Polyphenyl Ether," ASLE Trans., 153 (1975).
15. Broszeit, E. and Hess, F. J., "Discussion to "A Scanning Electron Microscope Study of Fracture Phenomena Associated with Rolling Contact Fatigue Failure," Wear, 17, 314 (1971).
16. Jones, W. R., Jr., "Spherical Artifacts on Ferrograms," Wear, 37, 193 (1976).

17. Stowers, I. F. and Rabinowicz, E., "Spherical Particles Formed in the Fretting of Silver," J. Appl. Physics, 43, 2485 (1972).
18. Doroff, S. W., et al., "Spherical Particles Produced by Erosion," Nature, 247, 363 (1974).
19. Rabinowicz, E., "The Formation of Spherical Wear Particles," Wear, 42, 149 (1977).
20. Dalal, H., et al., "Progression of Surface Damage in Rolling Contact Fatigue," SKF-AL74T002, SKF Industries, Inc. (AD-780453), King of Prussia, Pa. (1974).
21. Schatzberg, P. and Felsen, I. M., "Effects of Water and Oxygen During Rolling Contact Lubrication," Wear, 12, 331 (1968).

TABLE I - SUMMARY OF TYPES OF WEAR PARTICLES OBSERVED ON FERROGRAMS

	Type of wear debris	Morphology	Size range	Comments
Metallic	Normal rubbing wear particles	Asymmetrical flakes with smooth surfaces	<5 μm in major dimension <1 μm thick	Normally appear in strings
	Fatigue spall particles	Flat platelets with smooth surfaces, irregularly shaped perimeter	5 to 20 μm in major dimension 1 to 2 μm thick	
	Spheres	Spherical particles	1 to 10 μm in diameter	Most were <5 μm in diameter
Non-metallic	Friction polymer	Irregularly shaped patches	Variable (from a few μm to a few mm)	Two types
				I II
				Transmitted light
				Transparent Translucent
				Reflected white light
				Dark Light blue
				Reflected polarized light with crossed analyzer
				Not observed White

TABLE II. - SUMMARY OF FERROGRAM RESULTS (FAILURES)

(Failures) test	Sample time, hr	Composite Ferrogram density, percent area covered	Fatigue spall particles rating ^a	Normal rubbing wear particles rating ^a	Spherical particles total
F-1	23	4.0	0	+	2
	31	9.3	0	+	2
	47	4.6	0	+	1
	49	6.5	+	++	12
	74	2.2	+	+	2
F-2	20	8.9	0	+	1
	34	10.5	0	+	2
	50	12.9	0	++	1
	58	11.1	+	++	0
	74	4.0	++	+++	3
	76	6.3	+++	++	4
F-3	22	9.2	++++	+++	8
F-4	43	8.2	0	++	0
	63	2.5	0	+	1
F-5	6	10	0	+	1
	22	3.0	+	+	1
	30	6.9	0	+	1
	47	1.7	0	+	1
	54	3.5	0	+	1
	71	3.7	0	+	1
	78	.9	+	+	3
	81	5.1	0	+	1
F-6	8	9.9	+	++	4
	36	8.9	+	+++	2
	43	11.7	0	+++	2
	67	28	+++	++++	1
	74	10.3	++	+++	7
	76	13.7	+++	++++	22
F-7	18	12	+	+	1
	25	5.9	+	+	0
	32	13	+++	+	2
	49	5.4	++++	+	6
	56	5.3	+++	+	0
	73	10.4	+++	+	1
	80	15.9	+++	+	2
	93	1.1	++++	++	16
	98	8.4	++++	+++	48

^aNone 0, few +, several ++, many +++, very many ++++.

TABLE III. - SUMMARY OF FERROGRAM RESULTS (SUSPENSIONS)

(Suspensions) test	Sample time, hr	Composite Ferrogram density, percent area covered	Fatigue spall particles rating ^a	Normal rubbing wear particles rating ^a	Spherical particles total
S-1	66	3.5	0	0	0
	73	6.0	+	+	16
	89	5.5	+	+	1
	113	2.8	+	+	0
S-2	16	1.1	0	+	0
	40	^b ND	++	+	1
	54	2.7	+	+	0
	71	2.8	+	+	1
	95	ND	++	+	5
	100	ND	++	+	12
S-3	45	7.8	+	+	1
	69	1.4	+	+	0
	76	2.1	0	+	0
	100	6.9	0	+	3
	118	7.8	+++	+++	10
S-4	27	ND	0	+++	0
	49	ND	0	+	2
	57	ND	+	+	0
	73	ND	+	+	1
	81	ND	+	+	3
	103	ND	++	+	1
S-5	21	4.4	0	+	1
	46	11.4	0	+	29
	54	6.4	++	+	15
	60	5.3	+	+	5
	100	8.5	+	+	4
S-6	6	20.4	0	0	0
	29	12.6	++	+	3
	45	7.1	++	+	9
	52	10.8	0	+	0
	67	11.0	+	0	2
	113	7.7	0	+	1
S-7	64	5.2	++	+	1
	89	4.1	+++	+	4
	93	8.2	+	+	1
	101	7.8	++	+	1
S-8	42	3.6	+	+	0
	66	1.0	+	+	2
	90	2.4	0	+	0
	97	2.1	0	+	2
	100	12.7	+	+	0
^c S-9	25	3.3	+	+	5
	31	3.0	0	+++	6
	49	2.0	0	+++	1
	55	3.0	+	+++	3
	71	2.0	0	+	0
	75	1.0	0	+	1
	76	2.0	0	0	0
	100	1.0	0	+	3

^aFew +, several ++, many +++.^bND (not determined), none 0.^cLow stress, 3.4×10^9 Pa (500 000 psi).

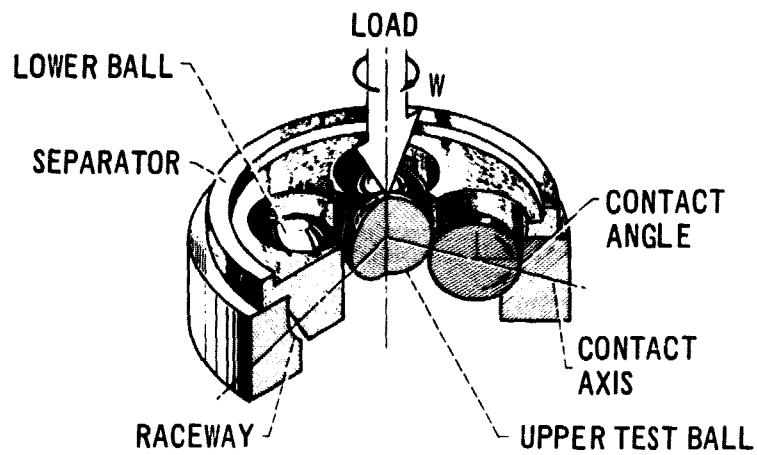


Figure 1. - Five-ball test assembly.

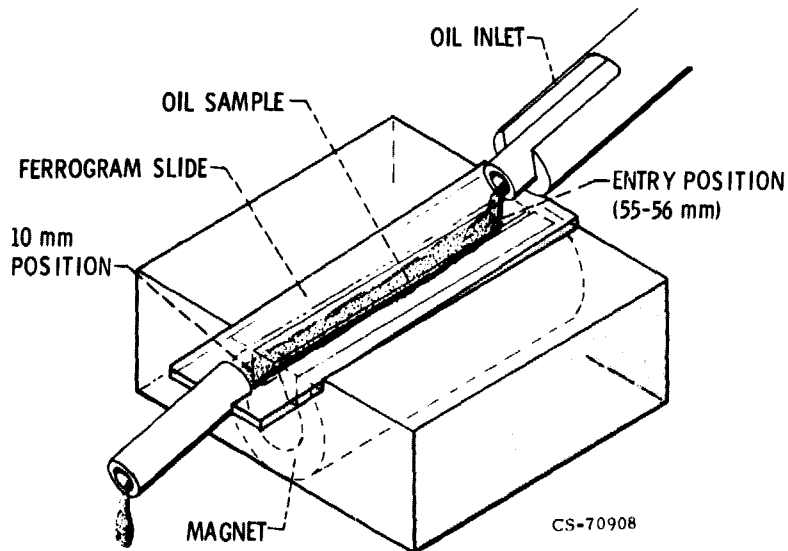


Figure 2. - Ferrograph analyzer.

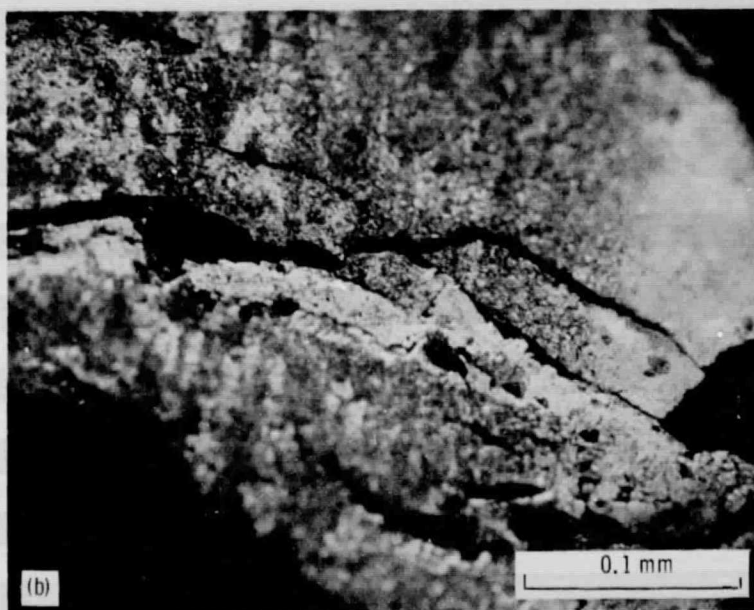
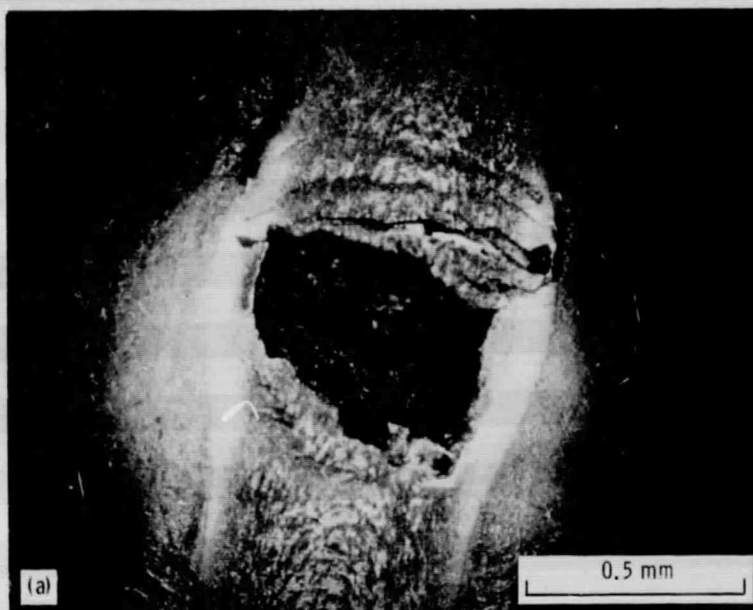


Figure 3. - (a) Typical fatigue spall. (b) Enlarged portion of (a).

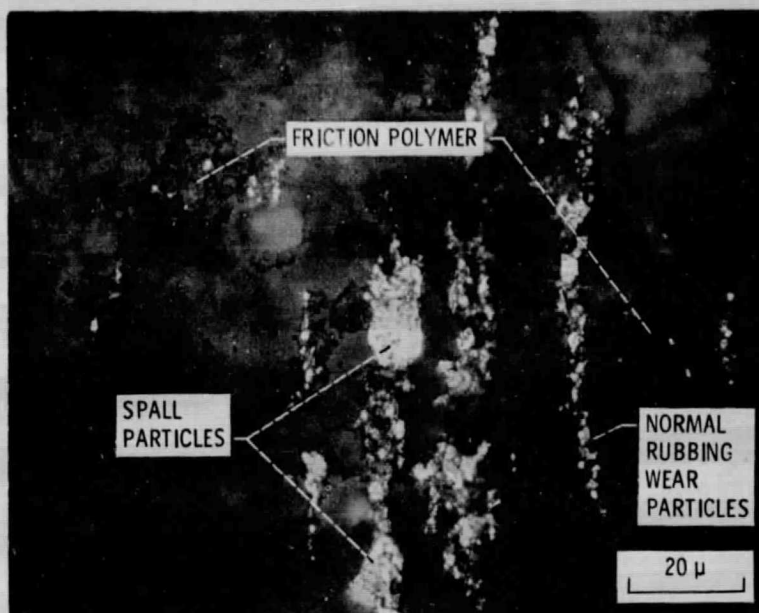


Figure 4. - Ferrogram entry deposit from test F-6 (76 hours).

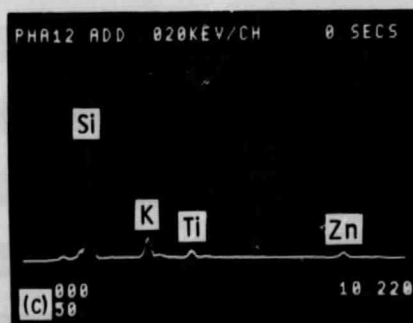
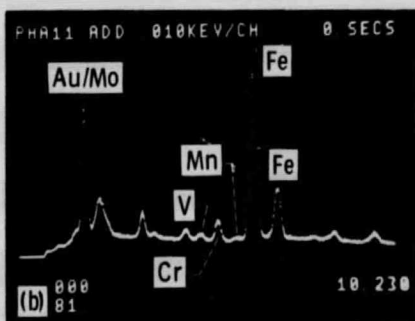
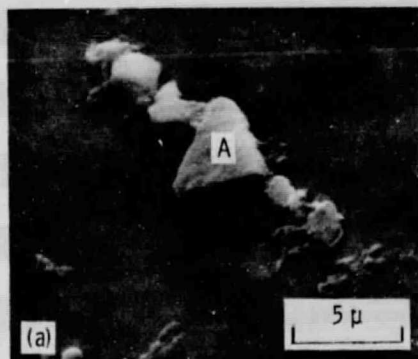


Figure 5. - (a) Electron micrograph of wear debris from test F-7 (98 hours), (b) energy dispersive x-ray analysis (EDAX) of particle A, (c) background EDAX of ferrogram.

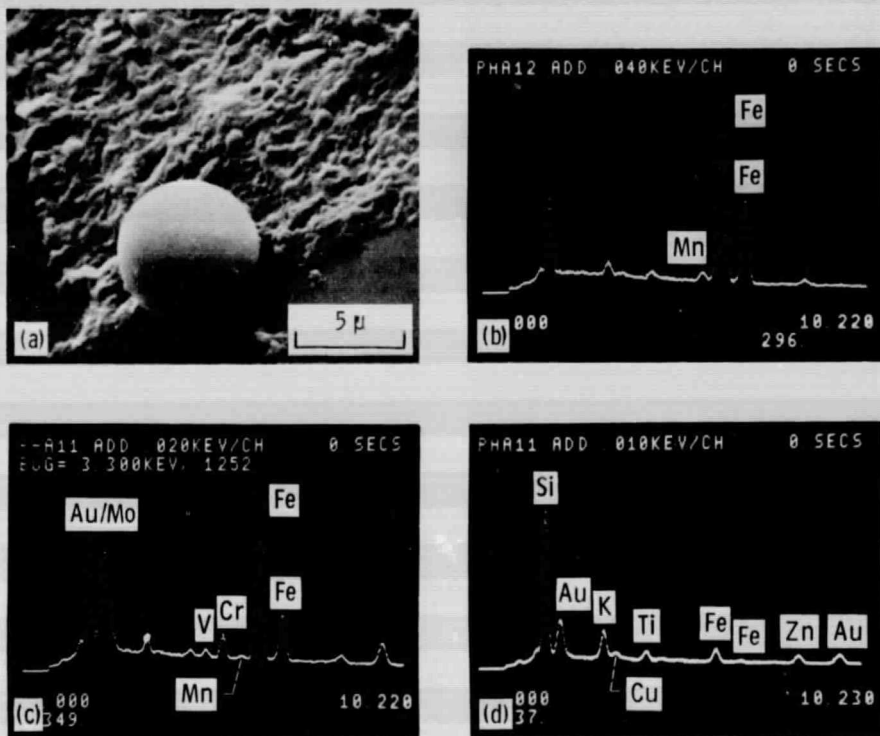


Figure 6. - (a) Electron micrograph of spherical particle and friction polymer from test F-7 (98 hours), (b) and (c) EDAX of spherical particles, (d) EDAX of friction polymer.

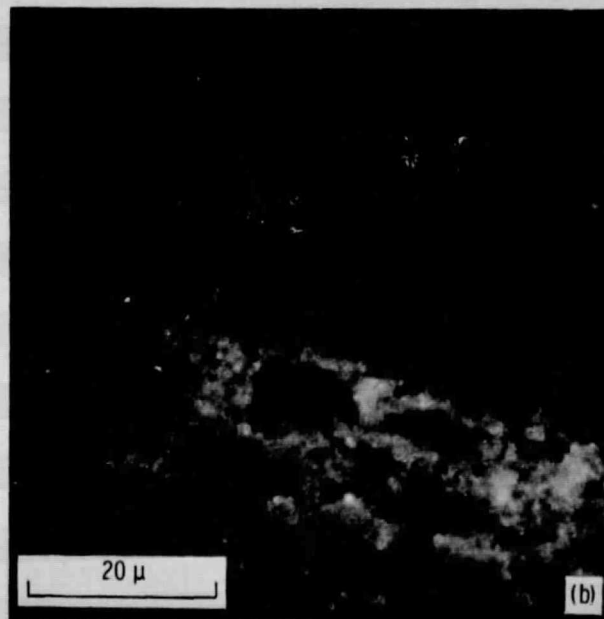


Figure 7. - Friction polymer deposit from test S-4 (27 hours). (a) Reflected light, (b) Reflected polarized light with crossed analyzer.

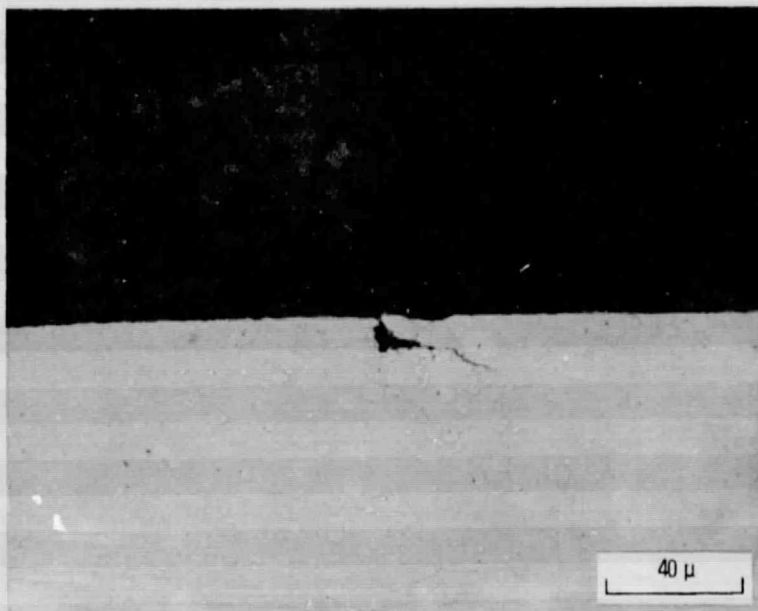


Figure 8. - Optical micrograph of sectioned wear track showing a surface crack (upper test ball, S-8, 100 hours).

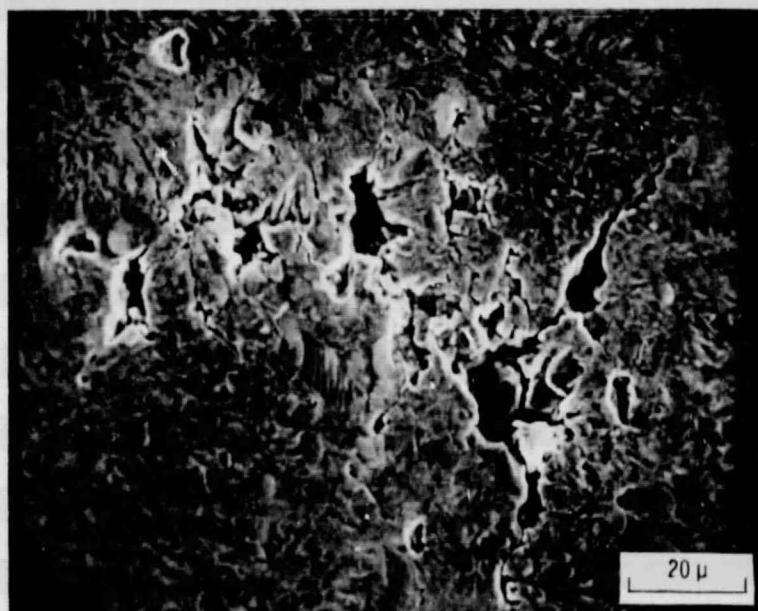


Figure 9. - Electron micrograph of wear track showing surface damage (upper test ball, S-5, 100 hours).